Marine Biology 61, 69–77 (1980)

MARINE BIOLOGY

Phytoplankton Sinking Rates in Oligotrophic Waters off Hawaii, USA

P. K. Bienfang*

Oceanic Institute; Waimanalo, HI 96795, USA

Abstract

The sinking rates in two size fractions of natural phytoplankton were measured over much of the photic zone in a subtropical environment. At 24, 40 and 71 m, sinking rates (± SD) of the 3 to 20 μm fractions were 0.72 ± 0.05, 0.83 ± 0.05, and 0.34 ± 0.04 m · d^{-1}, respectively, and rates for the 20 to 102 μm fraction were 1.50 ± 0.21, 1.65 ± 0.14, and 0.95 ± 0.22 m · d^{-1}, respectively. At all depths sampled, the 20 to 102 μm size fraction was observed to sink significantly ($P < 0.01$) faster than the 3 to 20 μm fraction. Considering vertical variability, both size fractions were observed to have significantly ($P < 0.01$) lower sinking rates at 71 m than at more shallow depths. The finding of lower sinking rates in the region which lies just above the subsurface chlorophyll maximum provides empirical support for the hypothesis that variations in phytoplankton buoyancy may be related to the maintenance of this feature which is typical in oceanic environments. Analysis of sinking rate traces describes the distributions of specific sinking velocities for each size fraction and their variation.

Introduction

Interest in phytoplankton sinking is centered around this phenomenon's proposed role in contributing to the downward flux of organic material and its influence on the vertical distribution of phytoplankton biomass and productivity (Steele and Yentsch, 1960; Semina, 1969, 1972; Smayda, 1970). The influence of phytoplankton sinking on the vertical transfer of photoautotrophic biomass accounts for the appearance of a sinking rate parameter in many ecosystem models, and the transport of chemical constituents to the ocean floor makes sinking of interest to sedimentologists. Phytoplankton sinking rates are dependent upon both physical (e.g., size and shape) and physiological phenomena (Munk and Riley, 1952; Smayda and Boleyn, 1966a, b; Hutchinson, 1967; Eppley *et al.*, 1967; Smayda, 1970; and others).

To date, most of the studies of phytoplankton sinking have dealt with populations maintained in the laboratory. By comparison, very little is known of sinking rates in nature, because most estimation methods either cannot be employed with heterogeneous populations and/or lack the sensitivity to monitor short time changes in the sparse biomass levels of natural systems. A recent study of heterogeneous populations in a Norwegian fjord (Lännergren, 1979), based upon data from settling columns, stands as the most intensive effort to describe buoyancy in natural populations. Difficulties with the accurate *in vitro* simulation of all parameters potentially influencing buoyancy in studies of unialgal cultures make the extrapolation of findings to the behavior of heterogeneous populations in nature difficult.

In view of the desirability to make sinking rate measurements on heterogeneous assemblages, a sinking rate method suitable for the analysis of field populations was developed (Rothwell and Bienfang, 1978; Bienfang, 1979). This technique, based upon measurement of the transit time of radioactively (^{14}C) labelled cells through a sinking column, was applied to the analysis of sinking rates in two size fractions throughout the photic zone in an oligotrophic environment. The site of this study (Lat. 19°55'N, Long. 156°10'W) is located 12 miles (ca 19 km) off Ke-ahole Point on the western side of the island of Hawaii, USA. It is a hydrographically deep station, a location of intensive phytoplankton studies, and has been shown to support phytoplankton stocks typical of open ocean subtropical areas.

* Oceanic Institute Contribution No. 162

0025-3162/80/0061/0069/$01.80

Materials and Methods

Water samples were collected using Niskin bottles, and corrected depths calculated from reversing thermometer data. All sampling was done prior to sunrise to avoid light shock to the phytoplankton. Collected samples were immediately transferred to a temperature-controlled (18 °C) room and promptly subjected to gentle reverse filtration (Dodson and Thomas, 1964; Holm-Hansen *et al.*, 1970; Harrison and Davis, 1977) to separate the size fractions; this process was completed within ca 1 h after collection. Whole water samples were passed serially through 102 μm and 20 μm mesh Nitex screens, followed by a 3.0 μm pore Nucleopore (14 cm diameter) filter. Slowly driven, "floating"-magnetic stirring bars (Markson, Inc.) were used to keep populations in suspension and off the filter during this process. To evaluate the possibility of physiological damage, the reverse filtration procedure employed had previously been examined in the laboratory and shown not to effect changes in the C/N, ATP charge, or phaeopigment:chlorophyll *a* ratios of test populations. For the various trials, the 3 to 20 μm and 20 to 102 μm samples were brought to final concentrations which ranged from 0.90 to 1.2 μg chlorophyll $a \cdot l^{-1}$ and 0.26 to 0.30 μg chlorophyll $a \cdot l^{-1}$, respectively.

The ^{14}C-labelled phytoplankton for sinking rate analyses were acquired from an incubation process similar to that used for measurement of primary productivity. Size-fractioned samples (100 ml) were injected with $H^{14}CO_3$ (ca) 1 μ Ci $\cdot$ ml^{-1}; ^{14}C solutions were prepared from sterile, aqueous stocks (New England Nuclear) brought to working activity levels by dilution with buffered (pH > 9.0) distilled water. Sample incubation took place throughout the day (ca 10 h) in an on-deck, water-cooled assembly. The incubation temperature was 27 °C for all samples; *in situ* temperatures at the collection depths ranged from 23.6 °C (70 m) to 26.7 °C (21 m). The light field in the incubator was made to simulate both the light intensity and spectral quality at the depths of the sample origin. The submarine spectral distribution was matched by Rohm and Haas (No. 2424) Plexiglas filters, matched to spectral data from Bienfang and Gunderson (1977). Simulated light intensities (quanta $\cdot$ s^{-1} $\cdot$ cm^{-2}) were calibrated using a Quantum Scalar Irradiance Meter (Biospherical Instruments) and matched to sample depth quantum flux levels which were determined with a Profiling Quantum Scalar Irradiance Meter (Biospherical Instruments, Inc.). For the samples from 24, 40, and 71 m, the simulated light fields were 49, 30, and 12% of the incident irradiation at 1 m, respectively. Incident light levels prevailing during the incubation period were monitored with a LI-COR (LI-500) integrator equipped with a 185M module and 190S sensor, and found to be 2.08 to 5.06 $\cdot$ 10^7 μE $\cdot$ m^{-2}.

Phytoplankton sinking rates were determined by the technique of Bienfang (1979), involving measurement of the transit time of radioactively (^{14}C) labelled cells through a settling column of known height. The technical approach in this sinking rate method is analogous to the fluorometric (Eppley *et al.*, 1967) and microscopic (Smayda and Boleyn, 1966a, b) techniques of the discrete sample layer category (Bienfang *et al.*, 1977) wherein a sample containing the phytoplankton is carefully layered onto the surface of a fluid column of slightly (+1.6 ‰ S) hypersaline water. Filtered (0.45 μm) water, taken from the depth of sample origin, was used for the column fluid so that the chemical environment during the sinking rate trials simulated the *in situ* conditions from which the samples originated. Sinking rate trials were performed in a temperature-controlled room (T = 25 °C); water temperatures at the depths of sample origin ranged from 23.7° to 26.7 °C. Since the ^{14}C-labelled cells from the incubations became available at the end of the day, the subsequent sinking rate trials were conducted in darkness for all samples; in addition to avoiding perturbation of diurnal rhythms, the performance of all trials in darkness provided identical yet representative conditions for all trials, irrespective of the depth of sample origin. The sinking rate trials took place over a period of approximately 5 h.

The apparatus employed in these measurements consists of an inverted, multichannel Geiger-Müller (GM) detection system, coupled to a microprocessor to simultaneously compile output from any or all of the GM chambers for teletype printout. The GM component is an array of eight, separately operable, upward facing chambers which are flushed with Q-gas (98.7% He, 1.3% iso-butane). Each of the GM chambers has detection windows made of 12.5 μm Kaptan, coated with 400 Å gold, and is held firmly in place by tightly fitting O-rings seated in dual function support rings which also support the settling columns. The settling columns which sit atop the GM chambers consist of precision ground Plexiglas cylinders having a functional height of 5 cm. The lower lip of the column is grooved to accommodate a tightly fitting O-ring that holds a Mylar membrane taut. This membrane contains the fluid within the settling column. When the settling chamber is seated in the support ring, the membrane just touches the window of the GM chamber. Technical aspects of the apparatus are given in detail in Rothwell and Bienfang (1978). Samples containing labelled phytoplankton were carefully introduced to the top of the column fluid using a peristaltic syringe to deliver steady flow-rate infusion required to maintain column stability. The upper lip of each settling column is internally bored to allow seating of airtight covers which minimize free surface area and enhance column stability. The sinking rate chamber array was supported in a two-dimensional gimbal suspension to dampen the effects of ship motion and this assembly was tuned as a low pass filter to attenuate propeller beat and vibrational modes up to 40 to 50 Hz.

For each depth, triplicate trials of both size fractions were performed simultaneously together with a control to verify that observed appearance of radioactivity at the chamber floor was due only to the passive sinking of labelled particulate material. Samples introduced to

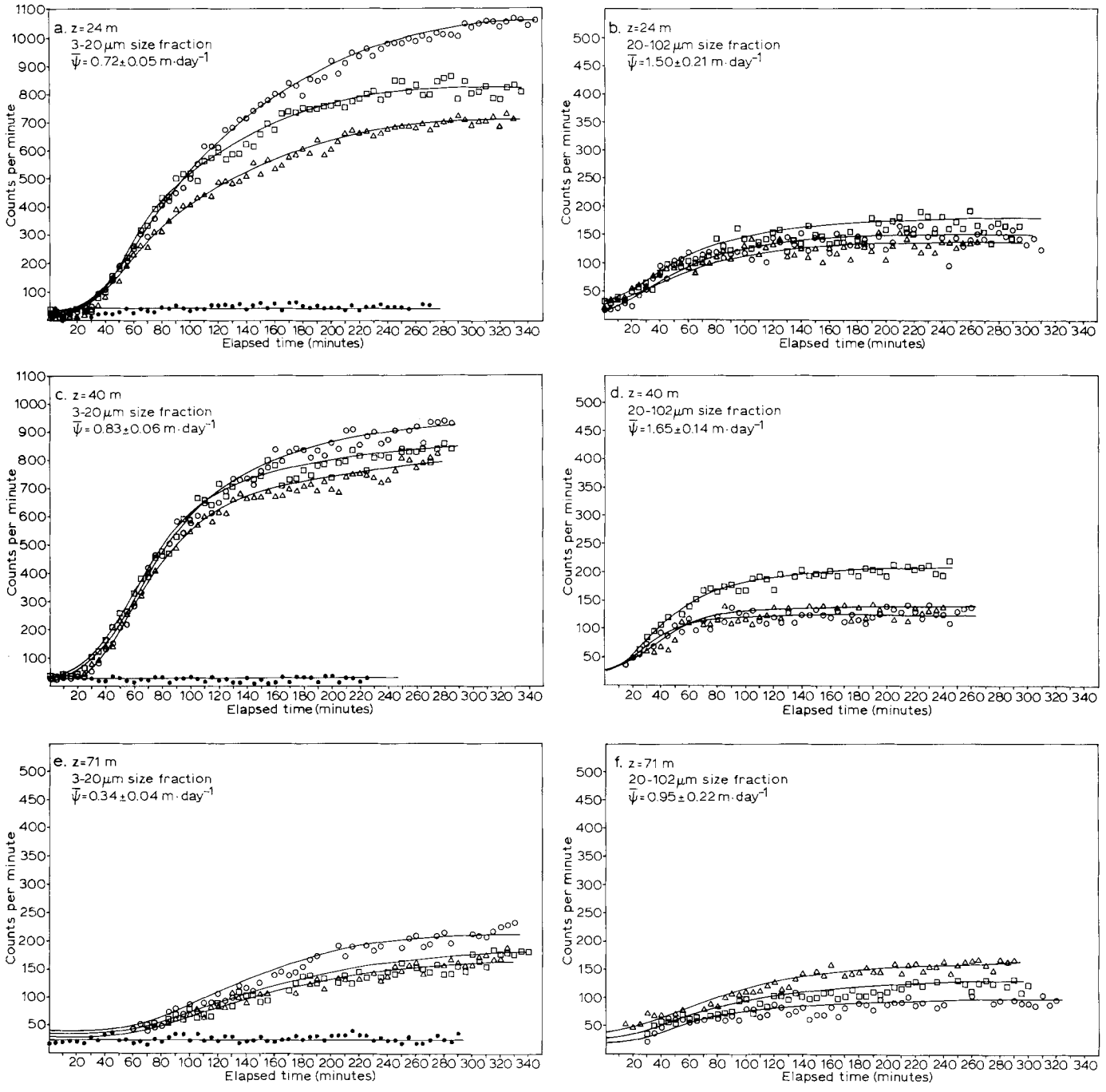

Fig. 1. Plots showing the arrival rate of radioactively labeled cells in samples from 3 depths over the photic zone of an oligotrophic system. The time-course distributions of triplicate sinking rate trials are shown for each size fraction together with the control trial (•) run with the samples from each depth

control columns consisted of filtered (0.45 μm) aliquots from the size fractioned samples; the time course of control trials (Fig. 1a, c, e), containing only dissolved ^{14}C, showed no detectable increase in activity over the duration of the sinking rate trials. Following trials, the final distributions of particulate ^{14}C and chlorophyll in the settling columns were measured to assess any population fraction which had not reached the sensed region. Calculation of sinking rates from the time-course distributions (Fig. 1) was done according to the mathematical framework for discrete-sample-layer methods. For each trial, the mean sinking rate, ψ, was calculated from the equation $\psi = h\phi/\ln(1 + h/l)$, where h and l are the heights of the sample and settling column cylinders, respectively, and $\phi = \int_0^\infty \frac{1}{t}\frac{df}{dt}\,dt$, where f is the

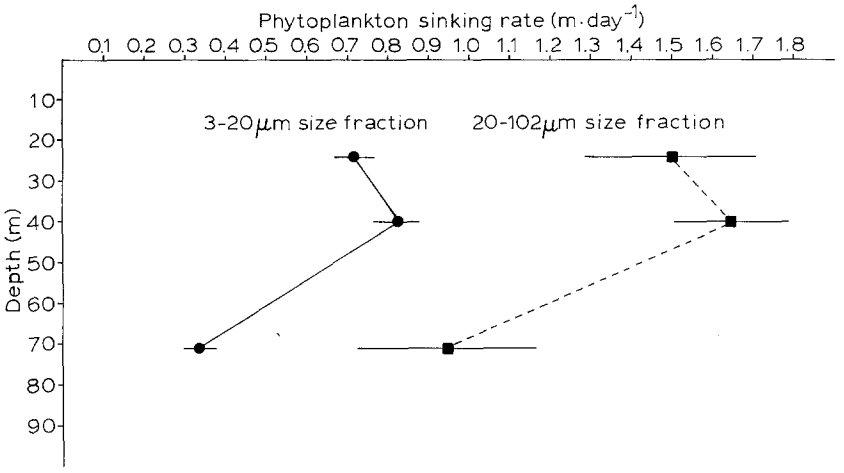

Fig. 2. Vertical distributions of phytoplankton sinking rates for the 3 to 20 μm and 20 to 102 μm size fractions, showing the mean (± SD) of triplicate trials for each depth. At 71 m the sinking rates in both size fractions were significantly ($P < 0.01$) lower than those measured higher in the water column

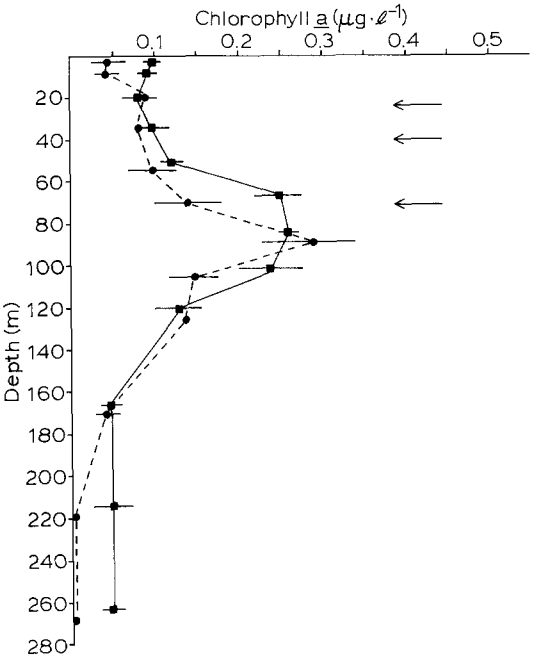

Fig. 3. Vertical distribution of chlorophyll from 2 hydrocasts taken at the time of sinking rate studies. Arrows indicate the depths sampled for sinking rate experiments

population fraction to have reached the bottom at time t, and comes from analysis of the time-course distributions (Fig. 1). The theoretical basis and mathematical derivation of these equations are given Bienfang *et al.* (1977).

For biomass analysis in the various size fractions, triplicate samples (chlorophyll *a*, phaeopigment, and ATP) were passed through filters having pore sizes of 0.45 μm (Gelman, cellulose acetate), 3.0 μm (Nucleopore, polycarbonate), and 20 μm (Nitex screen). Filtrations were done under low vacuum (e.g., 10, 2, and <2 cm Hg for 0.45, 3.0 and 20 μm pore sizes) to minimize artifacts in retention efficiency. Chlorophyll samples were measured using fluorometric techniques for extracted pigments (Strickland and Parsons, 1972). ATP samples were analyzed according to the methods of Karl and La Rock (1975) and Karl (1978) using an ATP photometer (SIA Corp.).

Results

Sinking rate plots for the 3 to 20 μm and 20 to 102 μm size fractions at 24, 40 and 71 meters are given in Fig. 1a to f. Plots show the arrival rates of radioactively (^{14}C) labelled cells, used in calculation of the mean sinking rate (ψ) in each trial; also given in the figures are the mean (± SD) values calculated from triplicates in each case ($\bar{\psi}$). For the 3 to 20 μm fraction, sinking rates ranged from 0.34 ± 0.04 to 0.83 ± 0.06 m · d^{-1}; in the 20 to 102 μm fraction, rates ranged from 0.95 ± 0.22 to 1.65 ± 0.14 m · d^{-1}. The coefficients of variation (s.d./$\bar{\psi}$) in these trials ranged from 0.07 to 0.23 and averaged 0.12, reflecting good reproducibility within the triplicate sets.

Irrespective of the depth in question, sinking rates of the 20 to 102 μm fraction were significantly ($P < 0.01$) greater than those of the 2 to 20 μm fraction (Student's *t*-test). Comparison of the rates of the two fractions averaged over all depths examined showed that the 20 to 102 μm fraction displayed sinking rates which were ca 2x those of the 3 to 20 μm fraction, illustrating the influence of particle size on sinking rates.

The sinking rate results for both size fractions are plotted against depth (Fig. 2) to show the variations in ψ vertically for the samples collected from 24, 40, and 71 m. Within either size fraction, sinking rates in samples from the upper 40 m region were statistically similar ($P > 0.05$) with depth. In the deeper (71 m) region, the sinking rates were much lower than those observed higher in the water column. These differences were significant ($P < 0.01$) in both size fractions of phytoplankton examined. The depth region in which the decreased sinking rates were observed is marked by increased chlorophyll levels relative to the overlying surface waters and occurs just above the subsurface maximum, which at the time of these trials was found to be at 88 m (Fig. 3). The cooccurrence of lower phytoplankton sinking rates and increased chlorophyll levels

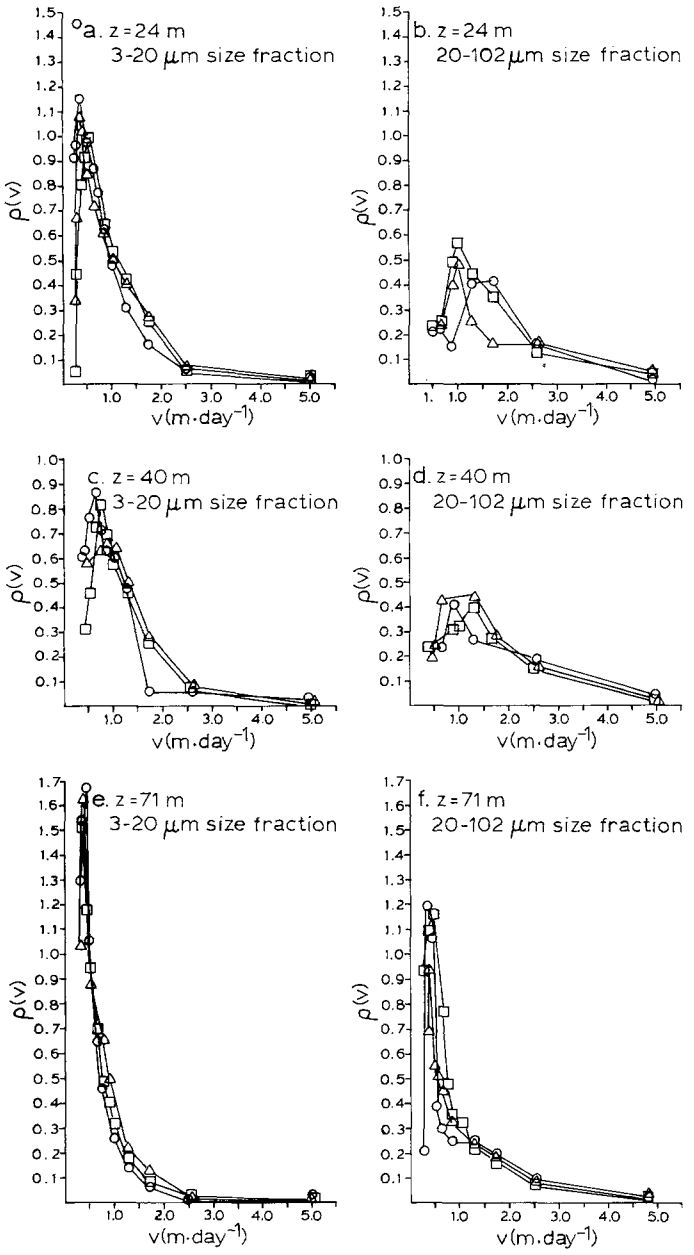

Fig. 4. Distribution functions [ρ(v)] of the sinking velocities calculated from the traces shown in Fig. 1 for the 3 to 20 μm and 20 to 102 μm size fractions from 24, 40, and 71 m

in this region indicates that phytoplankton buoyancy may be related to this characteristic feature of oceanic environments.

Fig. 4a to f shows the distributions of specific sinking velocities [ρ (v) $\cong$ (t^2/l) df/dt] in the two size fractions taken from 24, 40, and 71 m; ρ(v) is the sinking velocity distribution function, where the fraction of cells that sink at rates between V and V + dV is ρ(v)dV. The derivation of this equation comes from Equation (4) in Bienfang *et al.* (1977), and the distributions (Fig. 4a to f) are based on the first derivative of the time-course distributions (Fig. 1 a to f). All ρ(v) distributions have the shape of a skewed normal curve, reflecting the predominance of elements having low specific velocities constituting the curve mode, and the continually decreasing contribution of elements having higher sinking rates. Overall, the described V range extends from 5.0 m · d^{-1} to ca 0.2 m · d^{-1}; that the lower V bound does not extend to V = 0 reflects: (1) the practical inability to extend trials for infinitely long periods required to assess neutrally buoyant cells and (2) statistical constraints related to the handling of low slopes in the plateau region (Fig. 1a to f) which describes arrival rates of slow sinking elements.

The patterns of specific sinking rate distributions complement the mean population sinking rates calculated for these samples; both the location of the maxima and the relative area of the curves at higher sinking rates parallel variations in $\bar{\psi}$ (Figure la to f). The 3 to 20 μm samples show ρ(v) maxima (Fig. 4 a, c, e) at lower V than those for the 20 to 102 μm fractions (Fig. 4b, d, f). They also show considerably lower curve areas at higher V's, reflecting smaller contributions of faster sinking elements in the smaller size fraction. For either size fraction, the ρ(v) distributions appear similar between the populations from 24 m and those from 40 m, whereas both samples from 71 m show curve peaks at lower specific velocities and less curve area at higher specific velocities than were evident higher in the water column. The distributions of specific sinking rates indicate that the lower population siking rates observed in both fractions at 71 m were due to both smaller contributions of faster sinking elements and generally lower sinking rates in the cohorts having specific velocities constituting the curve mode.

The information given in Fig. 4a to f was further analyzed to describe the sinking rate distributions in terms of the percentage of the populations having sinking rates greater than various specific velocities (Fig. 5a to f). This was done by a computer formulation which calculated the area under the curve between two given specific velocities (i.e., the ρ(v)dV product), the % of the total area represented, and cumulative % curve area represented by all cohorts sinking faster than the lower bound of the dV interval in question. The results from each of the triplicate trials, described in Figs. 1 and 4a to f, were averaged and the mean (± SD) given by the data points and error bars shown in Fig. 5a to f. The differences in the relative contributions of faster sinking elements between the 3 to 20 μm and 20 to 102 μm size fractions are apparent in samples from all depths, and are most obvious in the pair originating from 71 m. Irrespective of depth, the curves describing the 3 to 20 μm size fractions (Fig. 5a, c, e) show lower % at higher sinking rates than their 20 to 102 μm counterparts (Fig. 5b, d, f), indicating that the observed size-related rate differences occurred as a result of differences over the entire range of specific sinking rates in these samples. For both fractions, the % distribution curves are similar between the 24 and 40 m comparisons (Fig. 5a and c, and b and d). Both the 3 to 20 μm and 20 to 102 μm samples from 71 m showed both lower contributions

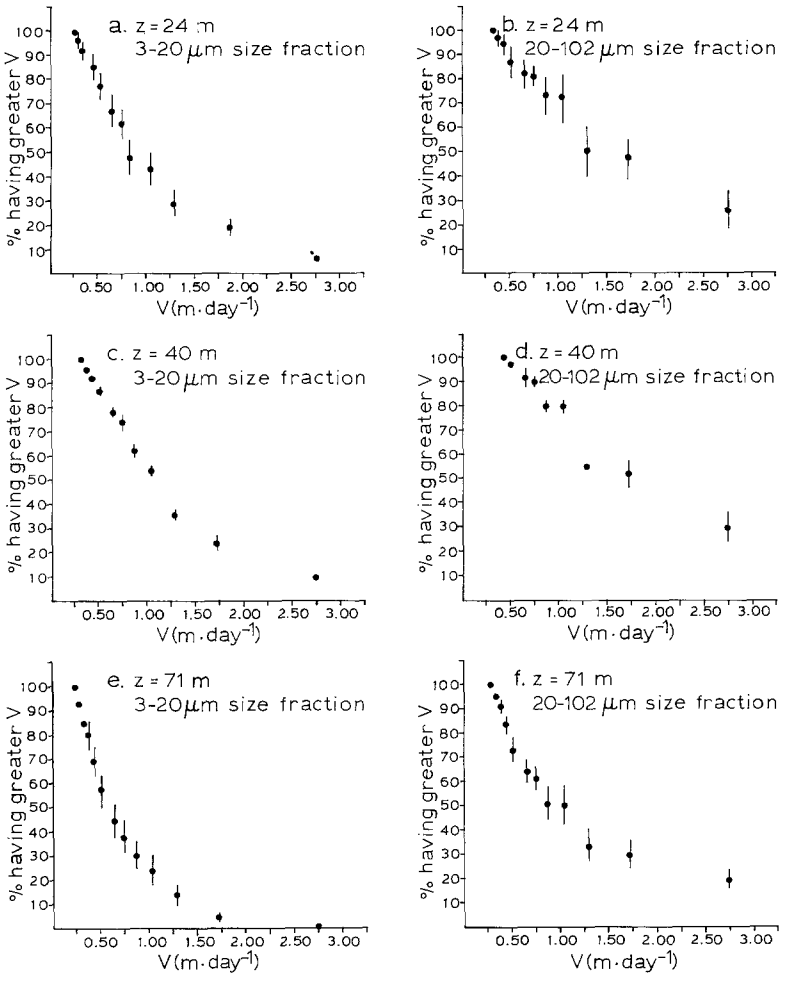

Fig. 5. Description of sinking rate distributions showing, for each set of triplicates, the mean (± SD) percentage of the population having sinking rates greater than various specific velocities

of faster sinking elements and more rapid curve decline than their counterparts originating from higher in the water column, suggesting that the lower mean sinking rates observed at 71 m arose from differences incurred throughout the entire range of specific velocities in these samples.

Discussion

One of the interesting possibilities afforded by the capability for sinking rate analysis on heterogeneous assemblages from the field is the inspection of buoyancy dynamics in the region of the deep chlorophyll maximum. Coinciding rather closely with the floor of the photic zone and the top of the pycnocline, this feature is typical of stable oceanic environments (Lorenzen, 1967; Saijo *et al.*, 1969; Hobson and Lorenzen, 1972; Venrick *et al.*, 1973; Jeffrey, 1976; Bienfang and Gundersen, 1977). Various explanations have been offered for this distributional phenomenon. Phytoplankton sinking rate deceleration has been suggested as an important parameter maintaining this distribution at the base of the mixed layer (Menzel and Ryther, 1959; Steele and Yentsch, 1960; Steele, 1961; Goering *et al.*, 1970; Venrick *et al.*, 1973; Jamart *et al.*, 1977). Increased cellular content of chlorophyll via adaptation to low prevailing light levels in the region has also been suggested as potentially capable of causing and/or reinforcing this distribution (Steele, 1962; Eppley *et al.*, 1973; Kiefer *et al.*, 1976; Jeffrey and Vesk, 1977). Although both mechanisms are based upon supportive laboratory and/or field data of various kinds, to date neither has had the benefit of empirical sinking rate observations made in the field. A subsurface chlorophyll maximum is a characteristic feature of the environment examined here. In twelve hydrocasts taken over the course of 14 months, the depth of this maximum ranged from 64 to 94 m, and was generally situated at ca 85 m (P. K. Bienfang and J. P. Szyper, in preparation). The vertical chlorophyll distribution at the time of these sinking rate studies (Fig. 3) showed the maximum at 84 to 89 m. Within the region around 71 m, the deepest location of sample origin for sinking rate analysis, the standing stocks of chlorophyll show increased levels relative to the overlying waters. The observation of substantially lower sinking rates in both the 3 to 20 μm and 20 to 102 μm fraction (Fig. 2) in this region of elevated chlorophyll levels just above the deep chlorophyll maximum represents the first set of empirical

Table 1. Distribution of chlorophyll *a*, phaeopipments, and ATP in various size fractions in the oligotrophic water column studied for sinking rates. Values give the % of total (collected on 0.45 μm pore size filters), and are based upon means of triplicates in each case

Depth (m)	Chlorophyll *a*			Phaeopigment			ATP	
	<3 μm	3–20 μm	>20 μm	<3 μm	3–20 μm	>20 μm	<3 μm	>3 μm
9	83.7	11.3	5.0	11.0	70.4	18.5	76.0	24.0
40	88.6	6.1	5.3	51.9	40.4	7.7	59.6	40.4
71	88.3	9.6	2.0	76.9	18.1	5.0	74.4	25.5
102	86.6	7.1	6.3	76.4	12.3	11.4	77.4	22.6
157	62.2	32.4	5.4	50.5	16.7	33.3	29.3	70.7

measurements showing a systematic co-variation of phytoplankton sinking rates and chlorophyll standing stocks. The lower sinking rates in the 71 m samples indicate support for the hypothesis that vertical variations in phytoplankton buoyancy may be involved in maintenance of subsurface chlorophyll maximum. It should be noted that the phytoplankton sinking rate information provided by this type of analysis does not translate unambiguously to net downward transfer rates. In the sea, the net vertical component of phytoplankton transfer is dependent on both the biological parameters controlling buoyancy and the physical processes of the water motion itself. This study gives evidence only that the behavior of the biological component near the region of the deep chlorophyll maximum would support the accumulation of biomass; whether the higher standing stock observed in this region actually results from this behavior depends in part on the co-occurring influence of physical processes.

To describe the population conditions in the environment in which the sinking rate measurements were made, samples from the various depths through the photic zone were assayed to show the prevailing size distribution of biomass. Filtration of samples from 9, 40, 71, 102 and 157 m through filters having mean pore sizes of 0.45 μm, 3.0 μm, and 20 μm showed most of the biomass to be found in the < 3.0 μm size fraction (Table 1). Chlorophyll analysis showed that contributions of the <3.0 μm, 3 to 20 μm, and >20 μm fractions to the total showed ranges of 62.2 to 85.6%, 6.1 to 32.4%, and 2.0 to 6.3%, respectively. The predominant contribution by the <3.0 μm fraction was also evident in the ATP data, which showed the <3.0 μm fraction to account for 29.3 to 77.4% of the biomass; ATP analyses were not done for the >20 μm case. In both biomass estimates, the relative contributions of the <3.0 μm fraction was lowest in the deepest (157 m) case, and were high and fairly uniform in the overlying waters. These data show the population in question to be dominated by small organisms. There is no data on the taxonomic composition of these samples or the sinking rates of the <3.0 μm fraction. Available data show sinking rates and their vertical variation in two size classes, accompanied by the relative contribution of those classes to the total. If it is reasonable to assume that the sinking rates of the <3.0 μm fraction would be lower than those measured for the >3.0 μm fractions, the net downward velocity of the entire population would be expected to be considerably lower than that shown for the 3 to 20 μm fraction.

Calculation of the maximum vertical mixing velocity in this area from the temperature and salinity distributions gave a rate of $3 \cdot 10^{-3}$ cm $\cdot$ s^{-1} (P. Falkowski, personal communication). Such an upward rate is sufficient to retain substantial portions of both the 3 to 20 μm and 20 to 102 μm size classes having specific sinking rate distributions shown in Figs. 3 and 4. Even mixing velocities lower by an order of magnitude could retain considerable proportions at the low end of the $\rho(v)$ distributions for either size fraction. The ramifications of chlorophyll retention brought about by the relative rates of water motion and particle sinking would be expected to be more pronounced with consideration of the <3.0 μm fraction as well.

Calculation of the mean sinking rate by the equations given in the Materials and Methods section is based upon the arrival rate of relative proportions of the total sample. Differences in the absolute value of the final plateau region among various trials reflect differing degrees of ^{14}C incorporation during the incubation period (due to varying biomass levels and these specific ^{14}C-incorporation rates); but because ψ is given by the arrival rate of population fractions, variations in the plateau signal *per se* do not affect the calculated sinking rate. Within any given trial, it is necessary to know that the biomass signal of the entire sample corresponds to the final plateau maximum. In the analysis of these trials, particular care was taken to normalize the final plateau signals to account for population elements which did not sink fast enough to reach the detection region within the trial period. This consideration can be very important in avoiding overestimation of the true mean sinking rates which would result if the apparent plateau maximum did not correspond to the signal of the entire population, i.e., analysis of only the faster sinking population elements. Within heterogeneous samples, both the relative contributions of various size fractions and the specific sinking rate distribution can influence the magnitude of the necessary normalization. In trials with the 3 to 20 μm fraction, the degree of plateau correction ranged from 8.8 to 22.0% and was generally about 8.9%; for the 20 to 102 μm trials, the correction ranged from 10.3 to 22.2% and was usually about 10.9%. Although addressing the relative contribution of comparatively small segments

of the total population, the accounting of any unmeasured, slow-sinking elements enhances the accuracy of the calculated mean sinking rates. The simultaneous analysis of triplicate trials of the two size classes from each depth allows the assignment of confidence limits to sinking rate values at any given depth, and minimizes the uncertainty of assuming equality of all buoyancy-influencing factors that would be encountered if independent measurements had to be made at different times. In these trials, replication allowed for the statistical comparison of sinking rate values both between the two size fractions and vertically for each fraction.

Indexing biomass arrival rates via recently assimilated ^{14}C focuses the sinking rate assessment on the photosynthetically active elements in a sample. Although the overall ^{14}C signal is irrelevant to the calculated ψ, the co-variance of specific incorporation rates among various segments represented in the distribution of specific sinking rates (Fig. 4) can have important ramifications since the average loss of photosynthetic products from a system depends on the ratio of both the specific incorporation and sinking rates of elements within a sample. The size fractionation via gentle reverse filtration has been shown not to alter metabolic activity within the sample (Harrison and Davis, 1977); this is relevant since physiological damage might influence the measured sinking rates. Development of the reverse filtration procedure used here included analysis of several indicators of the physiological status (e.g., C/N, ATP charge, phaeopigment/chlorophyll *a*) in concentrated samples and showed no evidence of pernicious effects to the population.

During trials, the stability of settling column fluid is a requisite demand for sinking rate assessments of this type at sea, and reflects the effectiveness of the gimbal operation, sample introduction, and the absence of column free surface area in maintaining nonturbulent conditions aboard ship. This was verified during those sinking rate trials by 3 separate types of observations. A "control" column, into which was introduced a filtered (0.45 μm) sample having only dissolved ^{14}C, was run together with the triplicate sets of the two size fractions from each depth. The absence of signal increase above normal background counts in these controls (Fig. 1) confirmed that the observed signal increases in sample trials were due solely to the appearance of labelled particulate material which had sunk through the sinking column to the region of detection. Secondly, a dye was added to this filtered sample so that the integrity of the introduced sample volume could be monitored visually both during sample introduction and throughout the trials. Observation of these dyed samples in the control columns, sitting adjacent to the trial runs, provided visual evidence of even sample layering and revealed the sample volume overlying the column fluid to remain intact throughout the trials, thus giving evidence of the absence of column turbulence. Thirdly, the final biomass (indexed both by chlorophyll and particulate ^{14}C) distribution in the columns at the ends of trials showed marked nonuniformity between settled and remaining pelagic fractions ($\geqslant$ 10:1), a condition which could not be evident if mixing were occurring within the columns.

Description of the distributions of specific sinking velocities (Figs. 4 and 5) provide information details of the buoyancy patterns within these samples, and gives a basis for inspecting intrasample variations of specific cohort velocities relevant to the different sinking rates calculated. It is interesting to note that both the 3 to 20 μm and 20 to 102 μm samples contained components which spanned a similar range of specific velocities (0 – 5.0 m $\cdot$ d^{-1}). Differences in the relative contributions of various component fractions in the $\rho(v)$ distribution, rather than pronounced differences in the absolute range of specific velocities, were primarily responsible for observed sinking rate differences. The lower overall sinking rates measured for the 3 to 20 μm fraction were shown not to be due solely to the absence of population elements sinking much faster than the mean but to intrasample differences which spanned most of the distribution of specific sinking velocities. That the low end of the $\rho(v)$ distributions does not extend to the ordinate reflects the analytical difficulty of direct assessment of the very slow sinking elements in a sample. Description of the distribution pattern relevant to the very slow sinkers represents an analytical difficulty involving both the trial duration (required to access the slowest elements directly), and the time frame of the df/dt regressions (required to give noise-free $\rho(v)$ patterns in the plateau region describing slow arrival rates). Fortunately the accuracy of calculated mean sinking rate does not suffer from this fact because the ψ calculation accounts for the presence and fractional contribution of these slow and/or neutrally buoyant cells.

Acknowledgments. This work was supported by Grants OCE75-03608-0A1 and OCE78-19234 from the National Science Fundation. I thank W. Johnson and D. Singer for their technical assistance at sea, and Drs. J. Szyper and E. Laws for their careful reviews of this manuscript. I am grateful to Dr. D. Karl for this performance of ATP charge ratios in evaluation of the reverse filtration procedures, to Dr. P. Falkowski for his calculation of the maximum mixing velocity, and to Captain O. K. Evans and the crew of the "Kana Keoki" for their efforts aboard ship.

Literature Cited

Bienfang, P.: A new phytoplankton sinking rate method suitable for field use. Deep-Sea Res. *26/6A*, 719–729 (1979)

Bienfang, P. K. and K. Gundersen: Light effects on nutrient-limited, oceanic primary production. Mar. Biol. *43*, 187–191 (1977)

Bienfang, P., E. Laws and W. Johnson: Phytoplankton sinking rate determination: Technical and theoretical aspects, an improved methodology. J. exp. mar. Biol. Ecol. *30*, 283–300 (1977)

Dodson, A. N. and W. H. Thomas: Concentrating plankton in a gentle fashion. Limnol. Oceanogr. *9*, 455–456 (1964)

Eppley, R. W., R. W. Holmes and J. D. H. Strickland: Sinking rates of marine phytoplankton measured with a fluorometer. J. exp. mar. Biol. Ecol. *1*, 191–208 (1967)

Goering, J. J., D. D. Wallen and R. M. Nauman: Nitrogen uptake by phytoplankton in the discontinuity layer of the eastern subtropical Pacific Ocean. Limnol. Oceanogr. *15*, 789–796 (1970)

Harrison, P. J. and C. O. Davis: Use of the perturbation technique to measure nutruient uptake rates of natural phytoplankton populations. Deep-Sea Res. *24*, 247–255 (1977)

Hobson, L. A. and C. J. Lorenzen: Relationship of chlorophyll maximum to density structure in the Atlantic Ocean and Gulf of Mexico. Deep-Sea Res. *19*, 297–306 (1972)

Holm-Hansen, O., T. T. Packard and L. R. Pomeroy: Efficiency of the reverse-flow filter technique for concentrating particulate matter. Limnol. Oceanogr. *15*, 832–835 (1970)

Hutchinson, G. E.: A treatise on limnology, Vol. II. Introduction to lake biology and the limnoplankton. 1115 pp New York: J. Wiley 1967

Jamart, B. M., D. F. Winter, K. Banse, G. C. Anderson and R. K. Lam: A theroretical study of phytoplankton growth and nutrient distribution in the Pacific Ocean off the northwest U. S. coast. Deep-Sea Res. *24*, 753–773 (1977)

Jeffrey, S. W.: A report of green algal pigments in the Central North Pacific Ocean. Mar. Biol. *37*, 33–37 (1976)

Jeffrey, S. W. and M. Vesk: Effect of blue-green light on photosynthetic pigments and chloroplast structure in the marine diatom *Stephanopyxis turris*. J. Phycol. *13*, 271–279 (1977)

Karl, D. M.: Occurrence and ecological significance of GTP in the ocean and in microbial cells. Appl. Environ. Microbiol. *36*(2), 349–355 (1978)

Karl, D. M and P. A. LaRock: Adenosine triphosphate measurements in solid and marine sediments. J. Fish. Res. Bd Can. *32*, 599–607 (1975)

Kiefer, D. A., R. J. Olson and O. Holm-Hansen: Another look at the nitrite and chlorophyll maxima in the Central North Pacific. Deep-Sea Res. *23*, 1199–1209 (1976)

Lännergren, C.: Buoyancy of natural populations of marine phytoplankton. Mar. Biol. *54*, 1–10 (1979)

Lorenzen, C. J.: A note on the chlorophyll and phaeophytin content of the chlorophyll maximum. Limnol. Oceanogr. *12*, 482–483 (1967)

Menzel, D. W. and J. H. Ryther: The annual cycle of primary production in the Sargasso Sea off Bermuda, pp 845–846. *In*: Preprints, International Oceanographic Congress, AAAS, Washington, D.C. 1959

Munk, H. W. and G. A. Riley: Absorption of nutrients by aquatic plants. J. mar. Res. *11*, 215–240 (1952)

Rothwell, G. N. and P. K. Bienfang: MARS - a new instrument for measuring phytoplankton siking rate. Mar. Technol. Soc. Journal 12, 13–17 (1978)

Saijo, Y., O. Iizuka and A. Asaoka: Chlorophyll maxima in Kuroshio and adjacent area. Mar. Biol. (Bull.) *4*, 190–196 (1969)

Semina, G. I.: The size of phytoplankton cells along longitude 174 °W in the Pacific Ocean. Am. geophys. U. Oceanology *9*, 391–398 (1969)

Semina, H. J.: The size of phytoplankton cells in the Pacific Ocean. Int. Rev. ges. Hydrobiol. Hydrogr., Bd. *57*, S. 177–205, (1972)

Smayda, T. J.: The suspension and sinking of phytoplankton in the sea. Oceanogr. Mar. Biol. Ann. Rev., H. Barnes (ed). *8*, 353–414 (1970)

Smayda, T. J. and B. J. Boleyn: Experimental observations on the flotation of marine diatoms. I. *Skeletonema costatum* and *Rhizosolenia setigera*. Limnol. Oceanogr. *11*, 18–34 (1966a)

Smayda, T. J. and B. J. Boleyn: Experimental observations on the flotation of marine diatoms. II. *Bacteriastrum byalinum* and *Chaetoceros landeri*. Limnol. Oceanogr. *11*, 35–43 (1966b)

Steele, J. H.: Primary production, pp 519–538. *In*: Oceanography. AAAS publ. 67, Washington, D.C. 1961

Steele, J. H.: Environmental control of photosynthesis in the sea. Limnol. Oceanogr. *7*, 137–150 (1962)

Steele, J. H. and C. S. Yentsch: The vertical distribution of chlorophyll. J. mar. biol. Assoc. U.K. *39*, 217–226 (1960)

Strickland, J. D. H. and T. R. Parsons: A practical handbook of seawater analysis. Bulletin 167, Fish. Res. Bd Can. (1972)

Venrick, E. L., J. A. McGowan and A. W. Mantyla: Deep maxima of photosynthetic chlorophyll in the Pacific Ocean. Fish. Bull. U.S. *71*, 41–51 (1973)

Date of final manuscript acceptance: September 30, 1980.
Communicated by R. O. Fournier, Halifax